Inorg. Chem. **2002**, *41*, 1807−1815

Carboxyester Hydrolysis Catalyzed by a Novel Dicopper(II) Complex with an Alcohol-Pendant Macrocycle

Shu-An Li, Jiang Xia, De-Xi Yang, Yan Xu, Dong-Feng Li, Mei-Fang Wu, and Wen-Xia Tang*

State Key Laboratory of Coordination Chemistry, Nanjing University, Nanjing 210093, People's Republic of China

Received October 1, 2001

A novel hexaaza macrocycle bearing two hydroxyethyl pendants (L), 3,6,9,16,19,22-hexaaza-6,19-bis(2-hydroxyethyl)-tricyclo[22,2,2,$2^{11,14}$]triaconta-1,11,13,24,27,29-hexaene, was synthesized as a potential binucleating ligand. The corresponding Cu(II) complex $[Cu_2LCl_2]Cl_2 \cdot 5.5H_2O$ was isolated as a blue crystal, triclinic, space group $P\bar{1}$, with $a = 9.4920(19)$ Å, $b = 4.783(3)$ Å, $c = 16.553(3)$ Å, $\alpha = 63.87(3)°$, $\beta = 86.10(3)°$, $\gamma = 83.8(3)°$, $V = 2072.8(7)$ Å^{-3}, $Z = 2$, R1 = 0.0658, and wR2 = 0.1839. Both Cu ions adopt the geometry of a distorted trigonal bipyramid in a pentacoordinated environment. A complexation study on the novel title complex has revealed that the alcoholic OH groups of the complex Cu_2L exhibit an obvious acidity with rather low pK_a values at 25 °C. The Cu(II)-bound alkoxides, which act as reactive nucleophiles toward the hydrolysis of 4-nitrophenyl acetate in 10% (v/v) CH_3CN at 25 °C, with $I = 0.10$ ($NaNO_3$) and pH 9.3, have shown a second-order rate constant, 0.41 ± 0.02 M^{-1} s^{-1}, a value that is approximately 10 times greater than the corresponding value for the mononuclear Cu(II) complex formed by a relatively simple tripodal ligand (L1). The pH–rate profile gave a sigmoidal curve. The possible catalytic mechanism has been proposed, and the reason for the high catalytic activity of the title complex has been discussed.

Introduction

In nature, some enzymes that promote phosphate ester hydrolysis, such as alkaline phosphatase and nuclease P1, are activated by two or more metal ions.[1] It is found that zinc ions work cooperatively in the catalytic hydrolysis. One of the zinc ions may polarize a nucleophile, e.g., either water or Ser-102 in the case of alkaline phosphatase, to attack an ester bond, while the other zinc ion can act transiently as a receptor for the leaving alcohol group. In the subsequent steps the role of these zinc atoms may be reversed.[2]

Recently, the synthetic metal complexes acting as model compounds for hydrolytic metalloenzymes have attracted much attention.[3−7] Much effort to design synthetic nucleases or alkaline phosphatase to elucidate the mechanisms by which metal ions promote hydrolysis has focused primarily on mononuclear Zn complexes and Cu complexes.[8−12] Kimura and co-workers studied the role of the alcohol pendant of the alcohol-pendant−[12]aneN_3−Zn(II) and alcohol-pendant−[12]aneN_4−Zn(II) complexes in the hy-

* To whom correspondence should be addressed. Phone: +86-25-3595706. Fax: +86-25-3314502. E-mail: wxtang@netra.nju.edu.cn.

(1) Sträter, N.; Lipscomb, W. N.; Klablunde, T.; Kreb, B. *Angew. Chem., Int. Ed. Engl.* **1996**, *35* (18), 2024−2055.
(2) Vallee, B. L.; Auld, D. S. *Acc. Chem. Res.* **1993**, *26* (10), 543−551.
(3) Perreault, D. M.; Anslyn, E. V. *Angew. Chem., Int. Ed. Engl.* **1997**, *36* (5), 433−450.
(4) Williams, N. H.; Takasaki, B.; Wall, M.; Chin, J. *Acc. Chem. Res.* **1999**, *32* (6), 485−493.
(5) Göbel, M. W. *Angew. Chem., Int. Ed. Engl.* **1994**, *33* (11), 1141−1143.
(6) Chin, J. *Acc. Chem. Res.* **1991**, *24* (5), 145−149.
(7) Wilcox, D. E. *Chem. Rev.* **1996**, *96* (7), 2435−2441.
(8) (a) Canary, J. W.; Xu, J.; Castagnetto, J. M.; Rentzeperis, D.; Marky, L. A. *J. Am. Chem. Soc.* **1995**, *117* (46), 11545−11547. (b) Xu, X.; Lajmi, A. R.; Canary, J. W. J. *J. Chem. Soc., Chem. Commun.* **1998**, 2701−2702.
(9) (a) Kimura, E.; Kikuta, E. *J. Biol. Inorg. Chem.* **2000**, *5*, 139−155. (b) Koile, T.; Kajitan, S.; Nakamura, I.; Kimura, E.; Shiro, M. *J. Am. Chem. Soc.* **1995**, *117* (4), 1210−1219. (c) Kimura, E.; Nakamura, I.; Koike, T.; Shionaoya, M.; Kodama,Y.; Ikeda, T.; Shiro, T. *J. Am. Chem. Soc.* **1994**, *116* (11), 4764−4771. (d) Kimura, E.; Shionoya, M.; Hoshino, A.; Ikeda,T.; Yamada, Y. *J. Am. Chem. Soc.* **1992**, *114* (26), 10134−10137.
(10) (a) Young, M. J.; Wajnon, D.; Hynes, R. C.; Chin, J. *J. Am. Chem. Soc.* **1995**, *117* (37), 9441−9447. (b) Chin, J.; Banaszczyk, M. *J. Am. Chem. Soc.* **1989**, *111* (7), 2724−2726. (c) Connolly, J. A.; Banaszczyk, M.; Hynes, R. C.; Chin, J. *Inorg. Chem.* **1994**, *33* (4), 665−669. (d) Chin, J.; Jubian, V. *J. Chem. Soc., Chem. Commun.* **1989**, 839−841. (e) Kim, J. H.; Chin, J. *J. Am. Chem. Soc.* **1992**, *114* (25), 9792−9795.
(11) Xia, J.; Xu, Y.; Li, S.; Yu, K.; Tang, W. *Inorg. Chem.* **2001**, *40* (10), 2394−2401.
(12) Hegg, E. L.; Mortimore, E. V.; Cheung, C. L.; Huyett, J. E.; Powell, D. R.; Burstyn, J. N. *Inorg. Chem.* **1999**, *38* (12), 2961−2968.

10.1021/ic011019l CCC: $22.00
Published on Web 03/14/2002

Chart 1

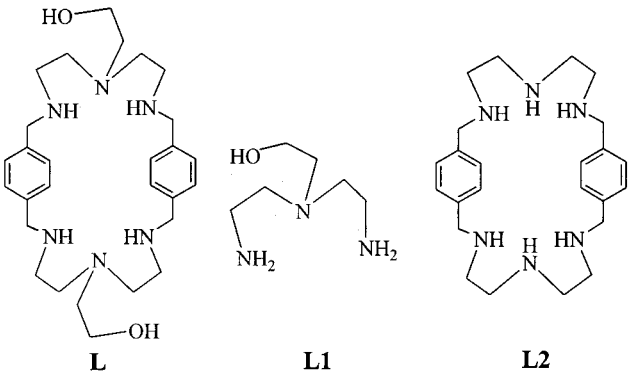

drolysis of carboxyl and phosphate esters. It was found that Zn(II)-assisted deprotonation of the alcohol pendant gives an RO−Zn(II) function, which is a better nucleophile than a Zn(II)−OH.[9b] Chin's group has investigated the reactivities and mechanisms of copper(II) hydroxide and copper(II) alkoxide for the cleavage of phosphate diester, and discovered that the copper(II) alkoxide-promoted transesterification path was 2 orders of magnitude faster than the hydrolysis path, i.e., the copper(II) hydroxide path.[10a]

However, few dinuclear metal complexes with macrocyclic ligands bearing hydroxyethyl pendants have been reported as models for alkaline phosphatases and nucleases.[13] Furthermore, enzymes always exhibit a certain degree of flexibility and can bind the substrate by an induced fit mechanism, whereas the biomimetic compounds are often too rigid or too flexible.[14] To mimic the cooperative mechanism between the adjacent metal ions and the effect of the flexibility of the structure of the enzymes, we have designed and synthesized a novel dinucleating ligand with two hydroxyethyl pendants containing *p*-xylyl spacers (see Chart 1, L) and its dicopper complex. The incorporation of the *p*-xylyl spacers into a macrocycle reduces the flexibility of the macrocycle.[15] In addition, we have strategically appended two hydroxyethyl groups to macrocycle L2, and hoped that the hydroxyethyl groups could be deprotonated upon the coordination of Cu(II) to give a strongly nucleophilic RO^-−Cu(II) species, which is able to act as a catalytic site in a fashion similar to that of the serine group in alkaline phosphatases. Here we describe the synthesis of the first alcohol-pendant macrocyclic ligand (L) and the crystal structure of the dinuclear Cu(II) complex of this ligand. The protonation constants of the ligand and stability constants of the Cu(II) complexes were investigated. The Cu(II) complex-catalyzed carboxylester hydrolysis was also studied.

Results and Discussion

Structure Description of $[Cu_2LCl_2]Cl_2\cdot 5.5H_2O$. The crystal structure of the dinuclear copper(II) complex consists of the cationic unit $[Cu_2LCl_2]^{2+}$, noncoordinated chloride ions, and crystallization water molecules. The crystal data and structural refinement parameters are displayed in Table 1. The selected bond lengths and angles are presented in Table 2. Figure 1 shows an ORTEP drawing of the structure of $[Cu_2LCl_2]^{2+}$ with 30% probability thermal ellipsoids. Each macrocycle binds two Cu(II) ions by its diethylenetriamine moieties, which provide three nitrogen donors to each Cu(II)

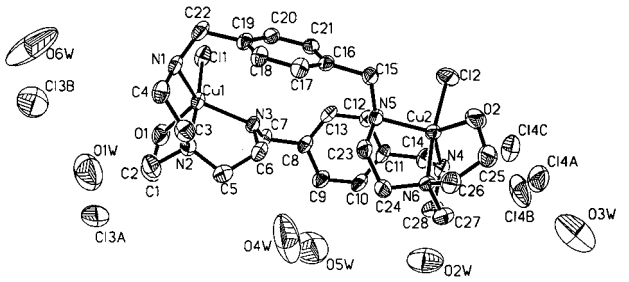

Figure 1. An ORTEP drawing (30% probability ellipsoids) of $[Cu_2LCl_2]^{2+}$. All hydrogen atoms are omitted for clarity.

Table 1. Crystal Data and Structure Refinement for $[Cu_2LCl_2]Cl_2\cdot 5.5H_2O$

empirical formula	$C_{28}H_{57}Cl_4Cu_2N_6O_{7.5}$
fw	866.68
temp	293(2) K
wavelength	0.71073 Å
cryst syst, space group	triclinic, $P\bar{1}$
unit cell dimensions	$a = 9.4920(19)$ Å, $\alpha = 63.87(3)°$. $b = 14.783(3)$ Å, $\beta = 86.10(3)°$. $c = 16.553(3)$ Å, $\gamma = 83.86(3)°$.
vol	2072.8(7) Å^3
Z, calcd density	2, 1.389 g/cm^3
abs coeff	1.331 mm^{-1}
$F(000)$	906
cryst size	0.28 × 0.26 × 0.24 mm
θ range for data collection	1.37−24.97°
limiting indices	$0 \le h \le 11$, $-17 \le k \le 17$, $-19 \le l \le 19$
no. of reflns collected/unique	7670/7202 ($R_{int} = 0.0351$)
completeness to $\theta = 24.97$	98.9%
abs correction	empirical
max and min transmission	0.7530 and 0.6870
refinement method	full-matrix least-squares on F^2
no. of data/restraints/params	7202/0/462
goodness-of-fit on F^2	1.065
final R indices [$I > 2\sigma(I)$]	R1[a] = 0.0658, wR2[b] = 0.1833
R indices (all data)	R1 = 0.1099, wR2 = 0.2217
largest diff peak and hole	0.812 and 0.456 e·Å^{-3}

[a] $R1 = \sum||F_o| - |F_c||/\sum|F_o|$. [b] $wR2 = [\sum w(|F_o|^2 - |F_c|^2)|/\sum|w(F_o)^2|^{1/2}$. $w = 1/[(F_o^2)^2 + (0.1276P)^2 + 2.6903P]$, where $P = (F_o^2 + 2F_c^2)/3$.

Table 2. Selected Bond Lengths (Å) and Angles (deg) for $[Cu_2LCl_2]Cl_2\cdot 5.5H_2O$

Cu(1)−N(2)	2.007(6)	Cu(2)−N(6)	2.028(5)
Cu(1)−N(1)	2.054(5)	Cu(2)−N(4)	2.055(5)
Cu(1)−N(3)	2.087(4)	Cu(2)−N(5)	2.116(4)
Cu(1)−O(1)	2.177(5)	Cu(2)−O(2)	2.186(5)
Cu(1)−Cl(1)	2.245(2)	Cu(2)−Cl(2)	2.231(2)
N(2)−Cu(1)−N(1)	86.6(2)	N(6)−Cu(2)−N(4)	85.1(2)
N(2)−Cu(1)−N(3)	85.5(2)	N(6)−Cu(2)−N(5)	84.89(19)
N(1)−Cu(1)−N(3)	129.74(19)	N(4)−Cu(2)−N(5)	123.7(2)
N(2)−Cu(1)−O(1)	80.6(2)	N(6)−Cu(2)−O(2)	80.3(2)
N(1)−Cu(1)−O(1)	121.4(2)	N(4)−Cu(2)−O(2)	127.2(2)
N(3)−Cu(1)−O(1)	106.04(19)	N(5)−Cu(2)−O(2)	105.2(2)
N(2)−Cu(1)−Cl(1)	173.22(16)	N(6)−Cu(2)−Cl(2)	171.52(16)
N(1)−Cu(1)−Cl(1)	95.99(17)	N(4)−Cu(2)−Cl(2)	97.63(17)
N(3)−Cu(1)−Cl(1)	97.55(16)	N(5)−Cu(2)−Cl(2)	100.09(15)
O(1)−Cu(1)−Cl(1)	92.73(18)	O(2)−Cu(2)−Cl(2)	91.73(17)

(13) Bazzicalpi, C.; Bencini, A.; Berni, E.; Bianchi, A.; Fedi, V.; Fusi, V.; Giorgi, C.; Paoletti, P.; Valtancoli, B. *Inorg. Chem.* **1999**, *38* (18), 4115−4122.
(14) Molenveld, P.; Engbersen, J. F. J.; Reinhouldt, D. N. *Chem. Soc. Rev.* **2000**, *29*, 75−86.
(15) Bazzicalupi, C.; Bencini, A.; Bianchi, A.; Fusi, V.; Giorgi, C.; Paoletti, P.; Stefani, A.; Valtancoli, B. *Inorg. Chem.* **1995**, *34* (3), 552−559.

ion, and the rest of the coordinated atoms are a chloride anion and an oxygen atom from the hydroxyethyl pendant. The Cu1 atom lies 0.20 Å above the trigonal equatorial plane formed by the N1, O1, and N3 with N1−Cu1−O1 = 121.4°, N1−Cu1−N3 = 129.7°, and N3−Cu1−O1 = 106.0°, while the two axial sites are occupied by N2 and Cl1 with N2−Cu1−Cl1 = 173.2°. The Cu2 atom lies 0.24 Å above the trigonal equatorial plane defined by the N4, O2, and N5 atoms with N4−Cu2−O2 = 127.2°, N4−Cu2−N5 = 123.7°, and N5−Cu2−O2 = 105.2°, while the two axial sites are occupied by N6 and Cl2 with N6−Cu2−Cl2 = 171.5°. According to Mutterties[16] and Galy,[17] the values of $\Delta = 0.29$ for Cu1 and $\Delta = 0.39$ for Cu2 indicate that the coordination geometries around the two copper ions are all distorted trigonal bipyramidal and the distortion of Cu1 is more obvious than that of Cu2. The two Cu(II) ions lie 8.22 Å apart. Two phenyl rings of the Cu(II) complex are rather close to each other, with the shortest distance 3.65 Å for C13···C21, and form a dihedral angle of 77.3° to each other. Two hydroxyethyl groups and two coordinated chloride ions are all located at the same side of the plane defined by the nitrogen atoms of the macrocyclic ligand. The separation of the two coordinated chloride ions is 8.12 Å. It is of interest to compare the present structure with that of the Cu(II) complexes with L1 and L2. In the Cu_2L complex, the Cu−O(alcohol) bond lengths (2.177 and 2.186 Å) are shorter than the Cu−O distance of 2.286 Å in CuL1,[18] which indicates that the Cu−O bond is stronger than that of the latter complex. Furthermore, the distance between the two Cu(II) ions (8.22 Å) in Cu_2L is longer than that in $[Cu_2L2(CH_3CO_2)_2]$ (6.78 Å)[19] and $[Cu_2L'Cl_2]$ (6.95 Å),[15] in which L′ is a similar macrocyclic ligand, 1,4,7,16,19,22-hexamethyl-1,4,7,16,19,22-hexaaza[9.9]paracyclophane. Therefore, the presence of hydroxyethyl pendants in L makes the cavity size of the macrocycle vary to a high degree with respect to L2 and L′, and leads to a longer Cu···Cu distance as a result. Two kinds of hydrogen bonds occur in the structure. One of the hydrogen bonds is formed between N5 and O6W ($1 - x, -y, 1 - z$), N5···O6W = 3.20 Å, and N5−H5···O6W = 159.3°. The other kind of hydrogen bond exists between the secondary amino group of the ligand and the coordinated chloride, N1−H1···Cl1 ($-x, 1 - y, 1 - z$), N1···Cl1 = 3.36 Å, and N1−H1···Cl1 = 137.8°. Hydrogen bond interactions involving the alcohol OH are not found.

Protonation Constants and Stability Constants. The potentiometric curve for L·6HBr is illustrated in Figure 2. The titration curve of this ligand reveals that there is an inflection point at $a = 2.0$ (a = number of moles of added base per mole of ligand), which indicates that the two tertiary nitrogen atoms are of very low basicity and release their protons easily into aqueous solution at low pH. The buffer region occurring at higher pH corresponds to the neutralization of the remaining four ammonium groups of the ligand. The titration data were analyzed for equilibria 1−4. The protonation constants K_1–K_4 (α_{H^+} is the activity of H^+) are defined as follows:

$$L + H^+ \rightleftharpoons HL^+ \qquad K_1 = [HL^+]/[L]\alpha_{H^+} \quad (1)$$

$$HL^+ + H^+ \rightleftharpoons H_2L^{2+} \qquad K_2 = [H_2L^{2+}]/[HL^+]\alpha_{H^+} \quad (2)$$

$$H_2L^{2+} + H^+ \rightleftharpoons H_3L^{3+} \qquad K_3 = [H_3L^{3+}]/[H_2L^{2+}]\alpha_{H^+} \quad (3)$$

$$H_3L^{3+} + H^+ \rightleftharpoons H_4L^{4+} \qquad K_4 = [H_4L^{4+}]/[H_3L^{3+}]\alpha_{H^+} \quad (4)$$

The resulting calculated protonation constants of L in comparison with those of 2-[bis(2-aminoethyl)amino]ethanol are given in Table 3. The species distribution for the L·6HBr system is displayed in Figure 3a, and H_4L^{4+} predominates from pH 2 to pH 6.

The potentiometric titration data for the investigation of the complexation constants of L with Cu(II) are obtained by NaOH titration of L·6HBr in the presence of Cu^{2+} ions. In a solution containing Cu(II) (2.0 mmol) and L·6HBr (1.0 mmol), the titration curve reveals two inflections at $a = 6$ and $a = 8$, respectively, as shown in Figure 2. The inflection at $a = 6$ is remarkable, corresponding to the completion of the neutralization of the six ammonium ions in diethylenetriamine moieties that are easily deprotonated to form dinuclear complexes. The inflection at $a = 8$ indicates the deprotonation of another two titrable protons from $[Cu_2L]^{4+}$.

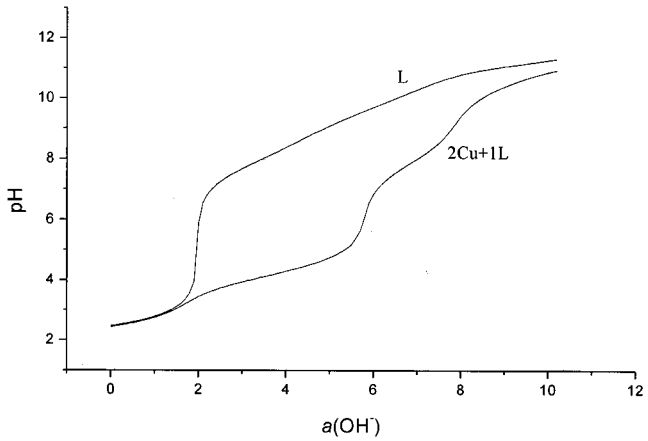

Figure 2. Potentiometric titration curves for L·6HBr and 2:1 molar ratios of Cu(II):L·6HBr (a = number of moles of NaOH added per mole of ligand, $I = 0.10$ M at = 25 °C).

Table 3. Comparison of Protonation Constants of L and the Relative Tripodal Ligand, Cu(II) Complexation Constants of the Two Ligands, and Deprotonation Constants of the Corresponding Complexes with $I = 0.1$ at 25 ± 0.1 °C

	L	L1		L	L1
log K_1	11.57	11.7[a]	log K(CuL)	15.57	15.68[b]
log K_2	8.96		log K(CuHL)	8.07	
log K_3	8.34	6.92[a]	log K(CuH$_2$L)	4.90	
log K_4	7.43		log K(Cu$_2$L)	6.64	
log K_5	<2	2.2[a]	pK_{a1}	7.60	8.5[b]
log K_6	<2		pK_{a2}	8.07	10.6[b]

[a] From ref 11. [b] From ref 18, $K_{a1} = [CuH_{-1}L1]\alpha_{H^+}/[CuL1]$. $K_{a2} = [CuH_{-1}L1(OH)]\alpha_{H^+}/[CuL1]$.

(16) Mutterties, E. L.; Guggenberger, L. J. *J. Am. Chem. Soc*. **1974**, *96* (6), 1748−1756.
(17) Galy, J.; Bonnet, J. I.; Anderson, S. *Acta Chem. Scand*. **1979**, *A33*(5), 383−389.
(18) Xia, J.; Li, S.; Shi, Y.; Yu, K.; Tang, W. *J. Chem. Soc., Dalton Trans*. **2001**, 2109−2115.
(19) Zhu, H. L.; Zheng, L. M.; Duan, C. Y.; Huang, X. Y.; Bu, W. M.; Wu, M. F.; Tang, W. X. *Polyhedron*. **1998**, *17* (22), 3909−3917.

Four major species, $[CuL]^{2+}$, $[Cu_2L]^{4+}$, $[Cu_2H_{-1}L]^{3+}$, and $[Cu_2H_{-2}L]^{2+}$, are believed to exist in aqueous solution, owing to the crystal X-ray analysis and electrospray mass spectrometry (ES-MS) experiments.

The complexation constants of L with Cu(II) ion, i.e., K and K_a, are defined as follows:

$$L + Cu^{2+} \rightleftharpoons [CuL]^{2+} \quad K(CuL) = [[CuL]^{2+}]/[L][Cu^{2+}] \quad (5)$$

$$[CuL]^{2+} + H^+ \rightleftharpoons [CuHL]^{3+}$$
$$K(CuHL) = [[CuHL]^{3+}]/[[CuHL]^{2+}]\alpha_{H^+} \quad (6)$$

$$[CuHL]^{3+} + H^+ \rightleftharpoons [CuH_2L]^{4+}$$
$$K(CuH_2L) = [[CuH_2L]^{4+}]/[[CuHL]^{3+}]\alpha_{H^+} \quad (7)$$

$$[CuL]^{2+} + Cu^{2+} \rightleftharpoons [Cu_2L]^{4+}$$
$$K(Cu_2L) = [[Cu_2L]^{4+}]/[[CuL]^{2+}][Cu^{2+}] \quad (8)$$

$$[Cu_2L]^{4+} \rightleftharpoons [Cu_2H_{-1}L]^{3+} + H^+$$
$$K_{a1} = [Cu_2H_{-1}L^{3+}]\alpha_{H^+}/[Cu_2L^{4+}] \quad (9)$$

$$Cu_2H_{-1}L^{3+} \rightleftharpoons Cu_2H_{-2}L^{2+} + H^+$$
$$K_{a2} = [[Cu_2H_{-2}L]^{2+}]\alpha_{H^+}/[[Cu_2H_{-1}L]^{3+}] \quad (10)$$

To rationalize the model selection and data process, several different analysis processes were conducted and evaluated. In the first case, the deprotonation species were set to be the dinuclear complexes $[Cu_2H_{-1}L]^{3+}$ and $[Cu_2H_{-2}L]^{2+}$; i.e., the species in eqs 5−10 were included. In the second case, the deprotonation species were set for both dinuclear and mononuclear complexes; i.e., the species in eqs 5−10 and $[CuH_{-1}L]^+$ were included. In the third case, all possible deprotonated species, and hydroxide species; i.e., the species in eqs 5−10 and $[Cu_2H_{-1}L]^{3+}$, $[Cu_2(OH^-)H_{-2}L]^+$, and $[Cu_2(OH^-)_2H_{-2}L]$ were included. In the first case, reasonable results were given by BEST, with a σ fit value optimized to be 0.025. However, in other cases, the additional species were calculated to be less than 1 ppm in concentration. Thus, we chose the first case as the most rational one.

Figure 3b displays the species distribution as a function of pH at a total Cu(II) concentration of 2 mM and total L concentration of 1 mM at 25 °C. The dinuclear complex $[Cu_2L]^{4+}$ is the predominant species over the pH range 5−7 (maximum at pH 6, 87.1%). $[Cu_2H_{-1}L]^{3+}$ and $[Cu_2H_{-2}L]^{2+}$ are the major complexes in solution at pH > 7. As demonstrated in Figure 3, the mono-deprotonated $[Cu_2H_{-1}L]^{3+}$ has a favorable pH of 7.6, above which it is gradually converted to $[Cu_2H_{-2}L]^{2+}$, and $[Cu_2H_{-2}L]^{2+}$ predominates at pH > 9. The structural formulas of the major species are displayed in Scheme 1.

ES-MS spectra for $[Cu_2LCl_2]Cl_2 \cdot 5.5H_2O$ were used to assist the investigation of the species in aqueous solution. The presence of the species with deprotonated hydroxyethyl pendants, $[Cu_2H_{-2}L]^{2+}$ (m/z = 311.3), is indicated with a relative abundance of 20% at pH 7 in Figure 4a. Peaks corresponding to hydroxide complexes are not found in this spectrum. The ES-MS spectrum for $[Cu_2LCl_2]Cl_2 \cdot 5.5H_2O$ at pH 8.5 is shown in Figure 4b. Besides the species $[Cu_2H_{-2}L]^{2+}$ with a relative abundance of 42% (m/z = 311.3) and $[Cu_2H_{-2}L\ (CH_3OH)_2]^{2+}$ with a relative abundance of 100% (m/z = 342.1), a weak peak at m/z = 685.1 assigned to the

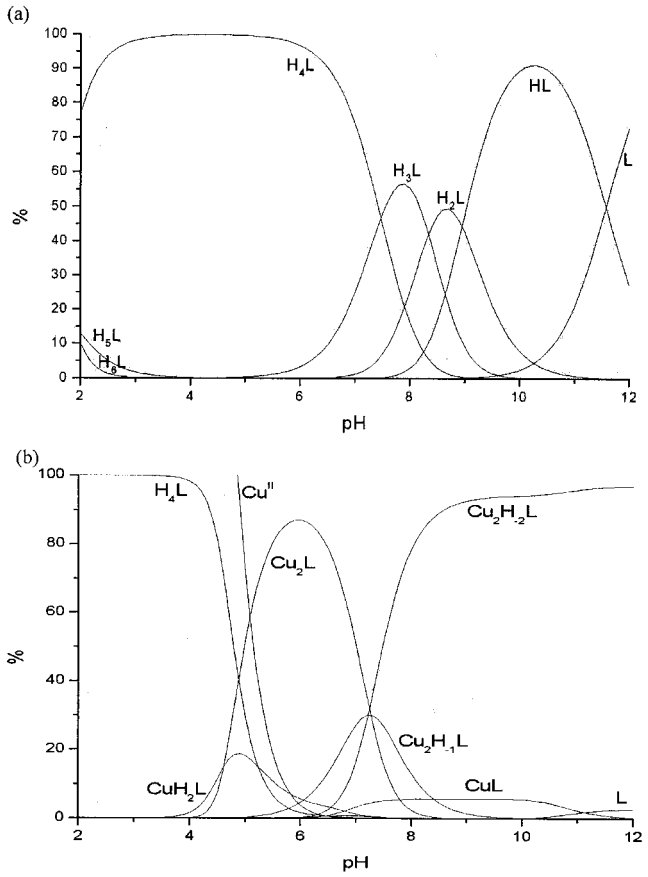

Figure 3. (a) Species distribution graph as pH for the 1.0 mM L·6HBr system at 25 °C and I = 0.1($NaNO_3$). (b) Species distribution graph as pH for the 1.0 mM L·6HBr + 2.0 mM Cu(II) system at 25 °C and I = 0.1-($NaNO_3$).

Scheme 1

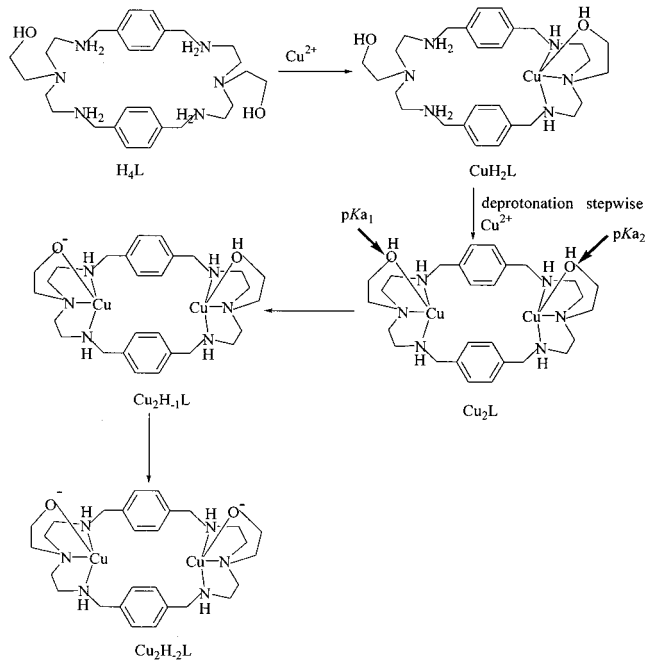

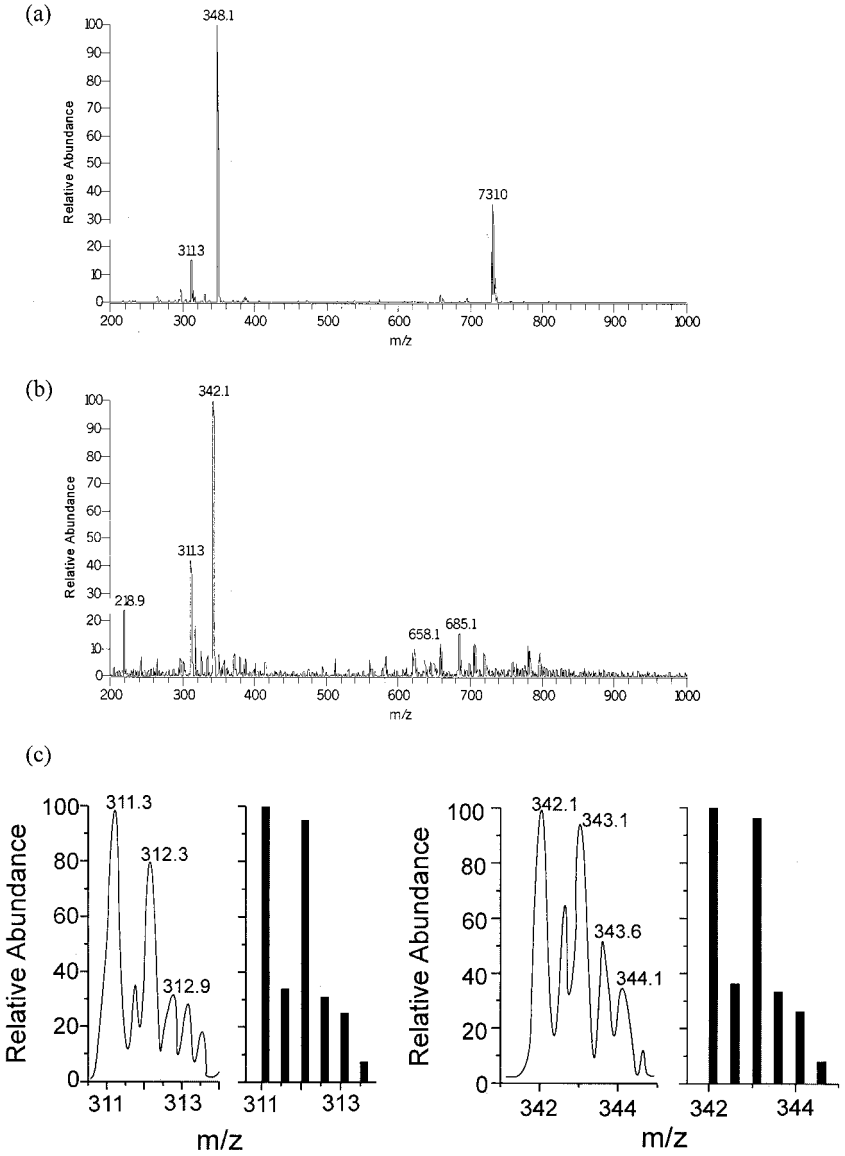

Figure 4. (a) Electrospray mass spectrum of the complex $[Cu_2LCl_2]Cl_2 \cdot 5.5H_2O$ at pH 7. The peak $m/z = 311.3$ is assigned to $[Cu_2H_{-2}L]^{2+}$, $m/z = 348.1$ to $[Cu_2LCl_2]^{2+}$, and $m/z = 731.0$ to $[Cu_2LCl_3]^{+}$. (b) Electrospray mass spectrum of the complex $[Cu_2LCl_2]Cl_2 \cdot 5.5H_2O$ at pH 8.5. The peak $m/z = 311.3$ corresponds to $[Cu_2H_{-2}L]^{2+}$, $m/z = 218.9$ to $[Cu_2LCl]^{3+}$, $m/z = 342.1$ to $[Cu_2H_{-2}L(CH_3OH)_2]^{2+}$, $m/z = 658.1$ to $[Cu_2H_{-2}LCl]^{+}$, and $m/z = 685.1$ to $[Cu_2H_{-2}L(CH_3OH)(CH_3O^-)]^{+}$. (c) Comparison of the observed (traces) and calculated (bars) isotopic distributions for the peaks at $m/z = 311.1$ and 342.1 in the ES-MS spectra of the complex.

alkoxide complex $[Cu_2H_{-2}L(CH_3OH)(CH_3O^-)]^{+}$ is observed. It indicates that the coordinated chlorides of the title complex can be substituted by CH_3OH and CH_3O^- when CH_3OH is used as eluent, and a substitution of Cl^- by OH^- and H_2O in water solution should be possible. All these species were confirmed by good agreement between the observed and calculated isotopic distributions. Figure 4c shows the typical examples for the comparison between the experimental and calculated isotopic distribution for the peaks at $m/z = 311.3$ and 342.1. The observed results mentioned above indicate that the deprotonation of hydroxyethyl bound to Cu(II) is much easier than that of a water molecule bound to Cu(II).

The obtained log K and the deprotonation constant pK_a for Cu_2L at 25 °C are listed in Table 3. The most significant finding is the rather facile deprotonation of the alcoholic function with $pK_{a1} = 7.60$ at 25 °C, which is lower than the value for the mononuclear CuL1 complex ($pK_{a1} = 8.5$) (Table 3). It is of interest to note the low pK_a value is close to that found by Kimura et al. for the Zn(II) complex with $pK_{a1} = 7.40$ at 25 °C[9c] and implies that the title complex is preferably a stronger nucleophile to attack an ester bond in catalytic hydrolysis.

The potentiometric investigation of equimolar Cu(II) ion and L·6HBr is also carried out by NaOH titration. There is an inflection at $a = 4$ in the 1:1 system, revealing that Cu(II) ion readily forms a mononuclear complex with the deprotonated ligand. The species concentration distribution as a function of pH depicted in Supporting Information Figure 1 indicates that the deprotonated species $[CuH_{-1}L]^{+}$ becomes predominant between pH 9 and pH 10.5.

4-Nitrophenyl Acetate Hydrolysis Catalyzed by the Cu_2L Complex. The activity of the Cu_2L complex in the catalytic hydrolysis of carboxylester has been investigated. Since the phosphomonoesters underwent slow hydrolysis

with Cu_2L similar to that of other Zn(II) or Cu(II) complexes, the carboxylester 4-nitrophenyl acetate (NA) was used as substitute.[9b,c,11] The hydrolysis of NA (0.25−2.0 mM) catalyzed by Cu_2L with concentrations varying from 0.25 to 2.0 mM at $I = 0.10$ and pH 7.3−9.3 in 10% (v/v) CH_3CN aqueous solution at 25 °C was followed by measuring the absorbance of released 4-nitrophenolate (NP) at 400 nm. The initial slope method was applied on the data processing procedure, as previously described in the literature.[8,9b,c]

To elucidate the mechanism of the present Cu_2L complex-catalyzed NA hydrolysis, we measured hydrolysis velocities both at constant NA concentration with varied total Cu(II) complex concentration and at constant total Cu(II) complex concentration with varied NA concentration. The blank hydrolysis process without the title complex as promoter was studied at each corresponding pH, which gave the spontaneous hydrolysis constant, known as ν_{buffer}. Initial velocities (ν_{total}) were measured by following the absorbance at 400 nm, increasing up to 5% of the extent of reaction. Since the concentrations of both the substrate NA and the promoter Cu_2L were essentially kept constant during the measurement, the absorbance increased linearly (correlation coefficient >0.99), with the slope being ν_{total}. The value of ν_{Cu2L} was obtained by eliminating the effect of the buffer as $\nu_{total} - \nu_{buffer}$. When the total Cu(II) complex concentration was set to be constant, the observed rate constant k_{obs} was calculated from the slope of the straight line $\nu_{Cu2L}/[\text{Cu(II) complex}]_{total}$ vs [NA]. This indicates that the rate is first order with respect to the substrate. On the other hand, at the same pH, when [NA] was set to be constant, k_{obs} was also measured in the presence of various concentrations of Cu_2L (0.25−2.0 mM). The plot of $\nu_{Cu2L}/[NA]$ vs $[\text{Cu(II) complex}]_{total}$ gave another straight line, with the slope denoted as k_{obs}, which testified that the rate is also first order with respect to the Cu_2L complex. Hence, we concluded that the Cu_2L-promoted hydrolysis is first order with respect to both the Cu_2L complex and NA, which is consistent with the previously reported Zn(II) complex-hydrolyzed carboxylester. The initial rate constant k_{in}, observed rate constant k_{obs}, and second-order constant k_{cat} are defined as follows:

$$\nu_{total} = \nu_{Cu2L} + \nu_{buffer} = k_{in}[NA]$$

$$\nu_{Cu2L} = k_{obs}[\text{Cu(II) complex}]_{total}[NA] = k_{cat}[Cu_2H_{-2}L][NA]$$

$$\nu_{buffer} = (k_{OH^-}[OH^-] + ...)[NA]$$

The second-order rate constant k_{cat} for Cu_2L is 0.41 M^{-1} s^{-1} at pH 9.3, calculated from the slope of the straight line k_{obs} vs $[\text{Cu(II) complex}]_{total}$ (see Figure 5) with the aid of the species distribution diagram, and the corresponding k_{cat} values of NA hydrolysis catalyzed by some other Cu(II) complexes are listed in Table 4. As indicated in Table 4, the $[Cu_2L]^{4+}$ complex is one of the most active catalysts for NA hydrolysis.

The first-order constants k_{cat} are plotted as a function of pH, and the resulting sigmoidal curve is shown as Figure 6. This indicates a kinetic process controlled by an acid−base

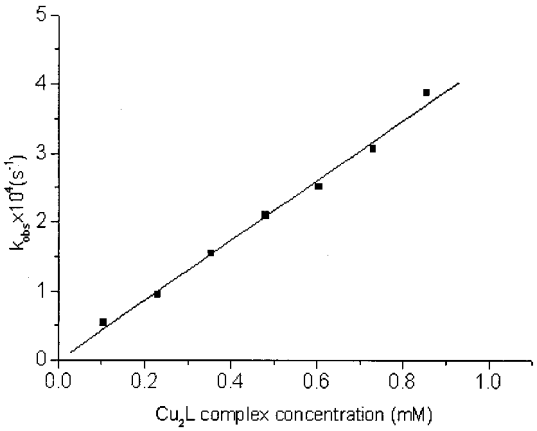

Figure 5. Typical dependence of observed pseudo-first-order rate constants for hydrolysis of NA on the total concentration of Cu_2L with $I = 0.1$ ($NaNO_3$ at 25 °C in the presence of 10% (v/v) CH_3CN, correlation coefficient >0.99.

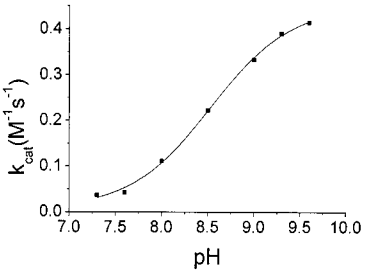

Figure 6. pH−rate profile for the second-order rate constants of NA hydrolysis with the Cu_2L complex at 25 °C and $I = 0.1$ ($NaNO_3$) in 10% (v/v) CH_3CN.

Table 4. Comparison of Hydrolysis Rate Constants, k_{cat} (M^{-1} s^{-1}), for Cu_2L and Other Complexes at $I = 0.1$ M ($NaNO_3$), pH 9.3, and 25 °C in 10% (v/v) CH_3CN

promoter[d]	k_{cat}	promoter[d]	k_{cat}
Cu_2L	0.41 ± 0.02	$[Cu(dipy)(H_2O)_2]$	0.16[a]
CuL	0.23 ± 0.01	CuL1	0.043[b]
Cu_2L2	0.027 ± 0.02	[12]aneN_3−Zn	0.14[c]

[a] From ref 10d. [b] From ref 18. [c] From ref 9c. [d] The actual nucleophiles are deprotonated Cu(II) complexes and a Zn(II) complex.

equilibrium, accelerated significantly when pH is over 7.8, which is consistent with the pK_{a1} (7.60) and pK_{a2} (8.07) values for the deprotonation of hydroxyethyl pendants of the title complex that were independently measured by potentiometric pH titration. Therefore, the promoter species are concluded to be the deprotonated species, $[Cu_2H_{-1}L]^{3+}$ and $[Cu_2H_{-2}L]^{2+}$.

To examine whether the whole process is catalytic hydrolysis or transesterification, we followed the release of NP up to more than one circle with NA concentration set to be 6.0 mM and Cu(II) complex concentration only 0.2 mM in buffer solution (pH 9.3) following the absorbance at 400 nm at 25 °C. The resulting ν_{total} vs time curve revealed that the rate constant for Cu_2L was identical to the initial rate constant determined above. Thus, the mechanism was catalytic hydrolysis.

To understand whether the cooperation exists between Cu(II) ions for binuclear Cu(II) complexes of L in the catalytic ester hydrolysis, we determined the rate constant of mononuclear Cu(II) complex (Cu:L = 1:1)-catalyzed NA hydroly-

Scheme 2

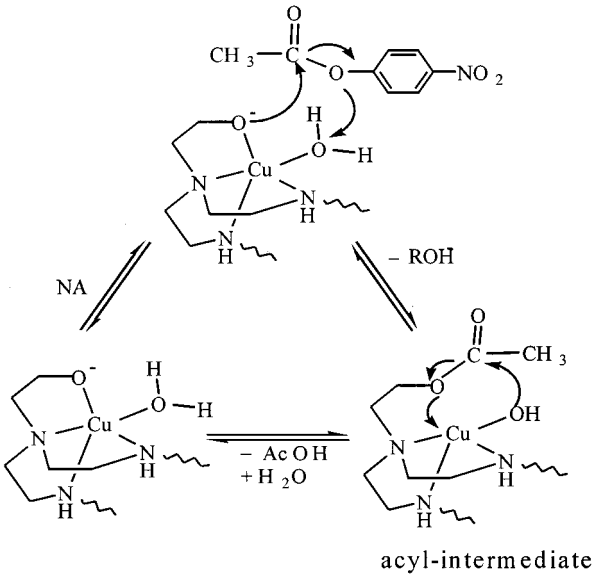

sis at the same conditions as that catalyzed by binuclear Cu(II) species (Cu:L = 2:1). The value was 0.23 M^{-1} s^{-1}, nearly half the value of Cu_2L, which demonstrates that each Cu(II) ion active center takes effect individually in catalytic hydrolysis of NA.

To further investigate the role of the hydroxyethyl pendants for the title compound in the catalytic ester hydrolysis, the rate constant of NA hydrolysis catalyzed by a Cu(II) complex with a macrocylic ligand without hydroxyethyl pendants (Cu_2L2) was also determined to give k_{cat} = 0.027 M^{-1} s^{-1} at pH 9.3, in which Cu(II)−OH is only an active nucleophile. Comparing the kinetic data for both Cu_2L and Cu_2L2, the rate constant of Cu_2L is approximately 15 times greater than the corresponding value of Cu_2L2 (see Table 4). These results suggest that a Cu(II)-bound alkoxide is a better nucleophile than a Cu(II)-bound hydroxide. On this basis, we suggest the possible overall reaction mechanism depicted in Scheme 2.[9,11]

First, the hydroxyethyl pendants bound to the Cu(II) ion at the active center deprotonate to yield a nucleophile to attack the electrophilic center of NA, while a hydrogen atom of the water molecule bound to Cu by substitution of the coordinated Cl^- acts as a receptor for the leaving groups. Then the Cu(II)-bound hydroxide acts as a nuclophile to attack the "acyl intermediate" to reproduce the active species to recycle the hydrolysis. It is worth pointing out that the rate constant of Cu_2L is approximately 10 times greater than the corresponding value (k_{cat} = 0.043 M^{-1} s^{-1}) of the CuL1 complex (see Table 4),[18] and for the individual Cu center, even near the corresponding value for the very reactive mononuclear alcohol-pendant−[12]aneN_3−Zn(II) complex. The greater catalyzed hydrolysis reactivity of Cu_2L compared to that of CuL1 may be due to the Cu−O bond length (2.18 Å) in the former complex being shorter than that in the latter complex (2.28 Å). As a result, the hydroxyethyl alcohol in the former complex can be easily deprotonated upon Cu(II) coordination with a lower pK_{a1} value of 7.6 to yield a strongly nucleophilic R−O^-−Cu(II) species. It may be due to the fact that the macrocyclic metal complex, especially benzyl and polar groups in the complex, construct the lipophilic and hydrophilic environment favorable of binding the substrate and stabilization leaving group. All these results help to explain the intrinsic role of the hydroxyethyl group in alkaline phosphatase hydrolysis.

Conclusion

A novel macrocyclic ligand with two hydroxyethyl pendants and its dicopper complex have been synthesized. The solution complexation study by potentiometric titration on the Cu(II) complexes of L has revealed that a stable 2:1 Cu(II) complex is formed, which has rather low pK_a values of 7.60 and 8.07 at 25 °C and I = 0.1 ($NaNO_3$). X-ray diffraction analysis of the title complex indicates that the Cu(II) ions adopt trigonal-bipyramidal geometry, the Cu−O bond lengths are longer than that of CuL1, and the Cu···Cu distance is longer than that of Cu_2L. ES-MS analysis of the aqueous solutions of the Cu(II) complex provided evidence for the existence of Cu(II)-bound alkoxide species. 4-Nitrophenyl acetate hydrolysis promoted by Cu_2L complex showed a second-order rate constant of 0.41 M^{-1} s^{-1}, which is approximately 10 times greater than that of the mononuclear copper complex of a relatively simple tripodal ligand (L1). The preference of the copper(II) alkoxide-catalyzed ester hydrolysis over copper(II) hydroxide-catalyzed hydrolysis was proved by kinetic experiments and shows evidence for the stronger nucleophilic ability of the copper(II) alkoxide than copper(II) hydroxide. In the catalytic reaction, the R−O^-−Cu(II) function acts as nucleophile in the first step of NA hydrolysis, giving an acyl intermediate, which is subsequently hydrolyzed via intramolecular attack of a Cu(II)−OH function. However, intermolecular attack by external water or hydroxide should not be ruled out.

Experimental Section

Instrumentation. C, H, and N analyses were made on a Perkin-Elmer 240C elemental analyzer. ^1H and ^{13}C NMR spectroscopic measurements were performed on a Brucker AM-500 NMR spectrometer. ES-MS spectra were recorded on an LCQ system (Finngan MAT) by injecting the diluted aqueous solution of the title complex using 1:1 methanol/water solvent as the mobile phase. The spray voltage and capillary temperature were set at 4.5 kV and 200 °C, respectively.

Syntheses. 2-[Bis(2-aminoethyl)amino]ethanol (L1) was prepared as described in the previous literature.[20] L2 was synthesized according to the procedure reported by Martell.[21] Other reagents were of analytical grade from commercial sources and were used without any further purification. The synthetic path of L and its Cu(II) complex is shown in Scheme 3. First L1 reacted with terephthaladehyde to give Schiff base, followed by reduction with $NaBH_4$ to yield L, and then the Cu_2L complex was synthesized by reaction of L and $CuCl_2$. These procedures are described below in detail.

3,6,9,16,19,22-Hexaaza-6,19-bis(2-hydroxyethyl)tricyclo-[22.2.2.2^{11,14}]triaconta-1,2,9,11,13,15,21,24,27,29-decaene. A solution of 98% terephthaladehyde (0.9973 g, 7.44 mmol) in MeCN (80 mL) was added dropwise to a stirred solution of 2-[bis(2-

(20) Bobylev, V. A.; Chechik, V. O. *Zh. Obshch. Khim.* **1990**, *60* (12), 2721−2725.
(21) Chen, D.; Martell, A. E. *Tetrahedron* **1991**, *47* (34), 6895−6902.

Scheme 3

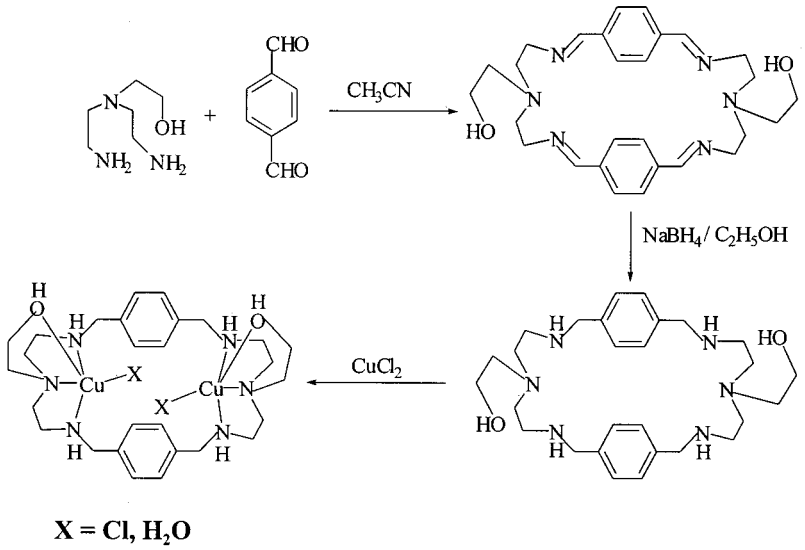

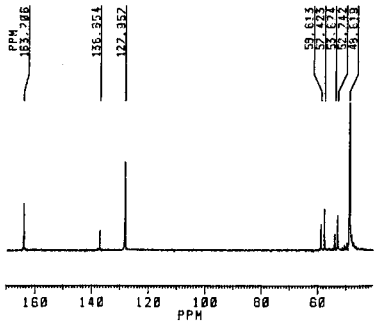

Figure 7. ^{13}C NMR spectrum of the macrocyclic Schiff base in CD_3OD/D_2O at 298 K.

aminoethyl)amino]ethanol (1.0937 g, 7.44 mmol) in MeCN (80 mL) at 0 °C over a period of 4 h. A white precipitate and an amount of sticky products were produced simultaneously after the reaction mixture was allowed to stir for additional an 12 h at 0 °C. The white precipitate was filtered out, and the filtrate was kept for several days at −5 to 0 °C. During the period at low temperature for crystallization, the sticky products and white precipitate appeared again, and the same procedure was repeated as mentioned above. All the solid products were combined and washed with MeCN, and dried in a vacuum desiccator over silica gel. The 500 MHz ^{13}C NMR spectrum of the product in CD_3OD/D_2O (in Figure 7) showed peaks at δ 53.7 and 58.6 (NCH_2CH_2OH), 52.8 and 57.5 (NCH_2CH_2N), 127.9 and 136.9 (phenyl), and 163.8 (CH═N), suggesting that the macrocyclic Schiff base is an expected product (yield 0.85 g, 1.74 mmol, 47%). ES-MS (4.5 kV, 200 °C): m/z = 491.3 for $[HL]^+$. Anal. Calcd for $C_{28}H_{38}N_6O_2 \cdot 2H_2O$ (526.7): C, 63.85; H, 8.04; N, 15.96. Found: C, 63.86; H, 7.97; N, 15.49.

3,6,9,16,19,22-Hexaaza-6,19-bis(2-hydroxyethyl)tricyclo-[22.2.2.2^{11,14}]triaconta-1,11,13,24,27,29-hexaene (L·6HBr and L). Sodium borohydride (0.5803 g, 15.39 mmol) was added in small portions to a suspension of the Schiff base (1.560 g, 4 mmol) in absolute ethanol (100 mL) with stirring at 45 °C. After the addition of the $NaBH_4$ was complete, the reaction solution was stirred for 10 h and then cooled. The reaction mixture was evaporated to dryness under reduced pressure. H_2O (3 mL) and CH_2Cl_2 (25 mL) were added to the mixture to extract the product. The organic phase was filtered, and the filtrate was evaporated to dryness. The residue was mixed with 48% HBr (3.0 mL) in an ice bath, the white precipitate formed was recrystallized from a mixture of H_2O/MeOH (5 mL/25 mL), and the product (L·6HBr) was dried in a desiccator over silica gel (yield, 2.78 g, 3.12 mmol, 78%). The 500 MHz ^{13}C NMR spectrum in D_2O gave peaks at δ 45.5 (CH_2 attached to phenyl), 52.1 and 55.6 (NCH_2CH_2OH), 52.7 and 59.2 (NCH_2CH_2N), and 128.5 and 138.1 (phenyl). Anal. Calcd for $C_{28}H_{46}N_6O_2 \cdot 6HBr$ (984.2): C, 34.17; H, 5.13; N, 8.56. Found: C, 34.03; H, 5.29; N, 8.29. The hexaaza macrocyclic ligand (L) was obtained according to the following method: Equivalent numbers of moles of L·6HBr and NaOH were dissolved in a small volume of water and cooled, and then CH_2Cl_2 was added to extract the product. A white powdery product was obtained when the organic phase was evaporated to dryness.

Dinuclear Copper Complex $[Cu_2LCl_2]Cl_2 \cdot 5.5H_2O$. To an aqueous solution (2 mL) containing $CuCl_2 \cdot 2H_2O$ (0.0341 g, 0.20 mmol) was added a solution of L (0.0498 g, 0.10 mmol) in H_2O (2 mL) dropwise with stirring at 60 °C. After being stirred for 10 min, the reaction mixture turned blue. A blue block single crystal was obtained for X-ray analysis by slow evaporation of the blue solution for several days at ambient temperature. Anal. Calcd for $Cu_2LCl_4 \cdot 5.5H_2O$ (866.7): C, 38.80; H, 6.63; N, 9.70. Found: C, 38.69; H, 6.33; N, 9.67.

X-ray Crystal Structure Determination. A blue crystal was mounted onto a glass fiber. The data collection was performed on the CAD4 X-ray diffractometer with graphite-monochromated Mo Kα radiation (λ = 0.71073 Å) using the $\omega/2\theta$ scan mode at 293 K in the range $1.37° \leq \theta \leq 24.97°$. The data were corrected for Lorentz and polarization effects during data reduction using XSCANS. The structure was solved by direct methods using SHELXS-97[22] and refined by full-matrix least-squares calculation on F^2 with SHELXL-97.[23] The uncoordinated chloride ions and crystalline water molecules were found disordered. The site occupancy factors for O5W and O6W were fixed at 0.75, Cl3A and Cl3B were fixed at 0.5, and Cl4A, Cl4B, and Cl4C were fixed at 0.5, 0.25 and 0.25, respectively. All non-hydrogen atoms were refined anisotropically. Full-matrix least-squares methods were used to refine an overall scale factor and positional and thermal parameters.

(22) Siemens, XSCANS (Version 2.1), Siemens Analytical X-ray Instruments, Madison, WI, 1994.
(23) Siemens, SHELXTL (Version 5.0), Siemens Industrial Automation, Analytical Instrumentation, 1995.

Potentiometric Determination. Potentiometric measurements of the protonation constants of the saturated hexaaza macrocyclic ligand L and the stability constants of its Cu(II) complexes were carried out with an Orion microprocessor ionalyzer-901 fitted with an Orion 91-04 glass combination pH electrode at 25 ± 0.1 °C. The ionic strength was 0.10 M, adjusted with $NaNO_3$. Solutions containing L·6HBr (1 mmol) with and without $CuSO_4$ (2 mmol) were titrated with carbon dioxide-free standard NaOH (0.10 M) solution to pH > 11. All solutions were carefully protected from air by a stream of humidified nitrogen gas. Standard NaOH was added by a spiral microinjector. The concentration of the $CuSO_4$ solution was calibrated by standard EDTA, and double-distilled water with a pH of about 6 was used. The temperature of the cell was controlled by a thermostat. The complexation and protonation constants were calculated using the program BEST.[24] In addition, solutions containing L·6HBr (1 mmol) with $CuSO_4$ (1 mmol) were also titrated, and the data were treated with the same program.

Kinetic Studies. The hydrolysis rate of NA catalyzed by Cu_2L was measured by an initial slope method in 10% (v/v) CH_3CN aqueous solution at 25 ± 0.5 °C as described previously for Zn−alcohol-pendant cyclen-catalyzed NA hydrolysis.[9b,c,11,25] Solutions containing Tris (20 mM) buffer (pH 7.3−9.0) or CHES buffer (pH 9.3−9.6) were used, and the ionic strength was adjusted to 0.10 M with $NaNO_3$. For the initial rate determination, the following procedure was employed. NA (0.25, 0.50, 0.75, 1.0, 1.50, 2.0 mM) and Cu(II) complex (0.25, 0.50, 0.75, 1.0, 1.5, 2.0 mM) were mixed in the buffer solution, and the UV absorption increase was recorded immediately at 400 nm on a Shimadzu UV-3100 spectrophotometer. The hydrolysis velocities were measured both at constant NA concentration with varied total Cu(II) complex concentration and at constant total Cu(II) complex concentration with varied NA concentration. To check whether the NA hydrolysis was catalytic, the substrate saturation kinetics were performed at pH 9.3 (buffered with CHES) and 25 °C with an ionic strength of 0.1 M (adjusted with $NaNO_3$). The NA concentration utilized was 6.0 mM, while the metal complex concentration was 0.2 mM for $[Cu_2L]^{4+}$. All the experiments were run twice, and the tabulated data represent the average of these experiments. The rates of hydrolysis for $[CuL]^{2+}$ and $[Cu_2L2]^{4+}$ are also measured at pH 9.3 in the same procedure mentioned above.

Acknowledgment. This work is supported by the National Natural Science Foundation of China.

Supporting Information Available: X-ray data in CIF format and figure showing the 1:1 metal−ligand species distribution graph. This material is available free of charge via the Internet at http://pubs.acs.org.

IC011019L

(24) Martell, A. E.; Motekaitis, R. J. *Determination and uses of stability constants*, 2nd ed.; VCH: New York, 1989.
(25) Suh, J.; Son, J.; Suh, M. P. *Inorg. Chem.* **1998**, *37* (19), 4872−4877.